Supporting Information

Targeted Radiosensitizers for MR-Guided Radiation Therapy of Prostate Cancer

Dong Luo,[†] Andrew Johnson,[‡] Xinning Wang,[§] Hao Li,[‡] Bernadette O. Erokwu,[†] Sarah Springer,[⊥] Jason Lou,[⊥] Gopalakrishnan Ramamurthy,[†] Chris A. Flask[†,∥] Clemens Burda,[⊥] Thomas J. Meade[‡,] and James P. Basilion[†,§,*]*

[†]Department of Radiology, Case Western Reserve University, Cleveland, Ohio 44106, United States

[‡]Department of Chemistry, Molecular Biosciences, Neurobiology, and Radiology, Northwestern University, Evanston, Illinois 60208, United States

[§] Department of Biomedical Engineering, Case Western Reserve University, Cleveland, Ohio 44106, United States

[∥]Department of Pediatrics, Case Western Reserve University, Cleveland, Ohio 44106, United States

[⊥]Department of Chemistry, Case Western Reserve University, Cleveland, Ohio 44106, United States

Experimental Section

Materials

All materials were supplied by Sigma-Aldrich unless otherwise stated, and used without further purification.

Synthesis and characterization of the Gd(III) and Y(III) complexes

The synthesis of the Gd(III) and Y(III) complexes proceeds via a convergent synthesis. The azido-labeled lipoic acid derivative (3-5(-azidopentyl) -1,2-dithiolane) and alkyne bearing DO3A derivative, are metallated with either Gd(III) or Y(III) coupled via copper(I)-catalyzed azide alkyne cycloaddition, as previously reported for the Gd(III) complex.[1] Briefly, Cu(II)SO_4, sodium ascorbate, and tris-hydroxypropyltriazolylamine were added to a 1:1:1 mixture of ethyl acetate, methanol, and water. To this solution was added 3-5(-azidopentyl) -1,2-dithiolane and the alkyne bearing DO3A derivative metallated with Gd(III) or Y(III). These complexes were purified by HPLC and the identity confirmed by analytical HPLC and high resolution ESI-TOF MS (Bruker AmaZon SL Ion Trap instrument).

Synthesis of the alkyne Gd(III) precursor proceeds from formation of N-propargyl acrylamide from propargylamine and acryloyl chloride. This acrylamide is then conjugated onto tert-butyl DO3A via an aza-Michael addition to yield the tert-butyl protected chelate. Following deprotection in 1:1 TFA and DCM, the chelate was metallated with $GdCl_3$. The alkyne-modified contrast agent was isolated by reverse-phase HPLC. Synthesis of the lipoic azide proceeds by reduction of lipoic acid to the alcohol with BH_3. The alcohol is converted to a tosylate group in situ, which is

subsequently displaced by sodium azide. The final lipoic azide is purified via silica gel chromatography

Synthesis of Au-Gd(III)-PSMA nanoparticles

AuNPs with core size of 5 nm were synthesized using a modified Brust-Schiffrin method.[2] After reaction, the DDA stabilized AuNPs were precipitated in pure ethanol and then re-suspended in chloroform. Concentration of AuNPs in chloroform was determined by UV-vis spectroscopy and a 1000 molar excess of Gd(III) complex was added to react with 1 equivalent of AuNP-DDA. The mixture was stirred over 24 h and then the solvent was evaporated at room temperature. The dried mixture was dissolved with PBS and un-conjugated Gd(III) complex was removed by extensive purification using centrifuge filters (MWCO=30 kDa, GE Healthcare). After purification, the Au-Gd(III) NPs were conjugated with Cys-PSMA-1 ligands with the same procedure with Cys-PSMA-1 added to Au-Gd(III) NPs at ratio of 40:1. After 24 h, un-conjugated peptides were removed by centrifugation with the 30 kDa filters. A similar procedure was used to generate Au-Y(III) NPs.

The hydrodynamic diameter of the Au-Gd(III)-PSMA NPs was characterized with a dynamic light scattering system (DynoPro NanoStar), and the AuNP core size was determined by transmission electron microscopy (FEI Tecnai F300 kV). Gel electrophoresis for PSMA-targeted Au-Gd(III)-PSMA NPs and untargeted Au-Gd(III) NPs was performed on 1% agarose gel and 1× TAE running buffer at 120 kV. Each chamber was loaded with 10 μL of 2 uM NPs, 5 μL of glycerol, and 5 μL of 4× TAE. All the NPs were pre-incubated with 10% fetal bovine serum (FBS) stained with coomassie brilliant blue (CBB) at 37℃ for 30 min. The stability of Au-Gd(III)-PSMA NPs in 10

% FBS and in PBS (pH at 5.5 and 6.5) was monitor by UV-vis spectrometry over one month, and release of Gd(III) from NPs was monitored by inductively coupled plasma mass spectrometry (ICP-MS, Agilent technologies, 700 series). Au-Y(III) NPs were characterized similarly.

Relaxivity and ICP-MS measurements

Quantification of Gd(III) and Au was performed using ICP-MS. For sample preparation, NPs were digested in aqua regia (25% nitric acid and 75% hydrochloric acid) overnight. The coverage of Gd(III) per AuNPs were determined according to the Gd(III)/Au ratio from ICP-MS measurement. Au atom number (N) per NP was calculated using the equation: $R= r_s \times N^{1/3}$ in which r_s represents the Wigner-Seitz radius (r_s=0.145 nm for Au) and R represents particle radius.[3]

Relaxivity of Au-Gd(III) NPs and Au-Gd(III)-PSMA NPs were measured on a 1.4 T NMR minispec (Bruker). Serially diluted NPs solutions were heated to 37℃ and placed into the Bruker minispec mq60 NMR spectrometer (60 MHz) to measure the T1 relaxation time. An inversion recovery pulse sequence with 3 averages, 15 s repetition time and 7 data points was used for data collection. The inverse of the longitudinal relaxation time (1/T1, s^{-1}) was plotted versus the Gd(III) concentration (mM), and the slope was defined as the relaxivity ($Mm^{-1}\ s^{-1}$).

Selective cell uptake

The selectivity of the Au-Gd(III)-PSMA NPs were determined by incubation with both the PSMA-positive PC3pip cells and PSMA-negative PC3flu cells. Cells were cultured in RPMI1640 medium with L-glutamine (2 mmol/L) and 10% FBS at 37 °C and 5% CO_2. To visualize the NP uptake,

cells were seeded in 8-well plates at 10^4 cells per well and then co-incubated with 50 nM Au-Gd(III)-PMSA NPs for 24 h. Culture medium was then removed and cells were washed with PBS, fixed with 4% paraformaldehyde, stained with silver staining kits (sigma), and imaged with a Leica DM4000B fluorescence microscope (Leica Microsystem Inc.).

The amount of Au and Gd(III) uptake by cells was determined by ICP-MS. Both PC3pip and PC3flu cells were seeded in 6-well plates at 10^5 cells per well and incubated for 24 h. Then cells were trypsinized, washed with PBS, and counted before digesting with aqua regia overnight. The digested cell suspensions were then diluted with DI water and measured with ICP-MS.

Binding affinity of Au-Gd(III)-PSMA NPs

LNcap cells were used to test the binding affinity of NPs. Specifically, LNcap cells were cultured in RPMI1640 medium, harvested, washed with 0.5 mM cold Tris buffer, and divided into 1.5 mL Eppendorf tubes at 5×10^5 cells per tube. The cells were then incubated with the ZJ24, free Cys-PSMA-1 ligands, and Au-Gd(III)-PSMA NPs at different concentrations in the presence of N-[N-[(S)-1,3-dicarboxypropyl]carbamoyl]-S-[3H]-methyl-L-cysteine (12 nmol/L, ^{3}H-ZJ24, GE Healthcare Life Sciences) in Tri buffer for 1 h at 37 ℃. All the tubes were then centrifuged and cells were washed three times with cold PBS. Finally, EcoLume cocktail (4 mL, MP biomedicals) was added to each tube, and radioactivity was counted with a scintillation counter. The concentration of ligands required to inhibit 50% of binding (IC_{50}) was determined using GraphPad Prism 3.0.

Cell pellet MR imaging

Both PC3pip and PC3flu cells were incubated with 50 nM Au-Gd(III)-PSMA NPs for 24 h and then harvested with trypsin, washed with PBS, and transferred to 5 3/4″ flame-sealed Pasteur pipets. The pipets were centrifuged again at 100 × g at 4.0 °C for 5 min to spin down the cell pellets. PC3pip and PC3flu cells without any NPs were used as the control. The samples were imaged using a RF RES 300 1H 089/023 quadrature transmit receive 23 mm volume coil (Bruker BioSpin, Billerica, MA, USA). For T1-weighted imaging, a spin echo sequence was used with the following parameters: TR = 500 ms, TE = 10 ms, flip angle = 90°, NEX = 3, FOV = 20 × 20 mm^2, slice thickness = 1 mm, and matrix size = 256 × 256.

***In vitro* cytotoxicity and radiosensitization**

Cytotoxicity of Au-Gd(III)-PSMA NPs and Au-Y(III)-PSMA NPs was evaluated with a CCK8 assay (Dojindo Molecular Technologies). Both PC3pip and PC3flu cells were cultured in 96-well plate and incubated with various concentration of NPs. Following a 24 h co-incubation, the medium was removed, and cells were washed with PBS. Fresh medium and CCK8 agent was added to each well. After 4 hours the 96-well plate was read at 450 nm (TECAN, infinite M200).

Radiosensitization of NPs was evaluated with a colony formation assay. Briefly, after incubating with 50 nM Au-Gd(III)-PSMA NPs or Au-Y(III)-PSMA NPs for24 h, the PC3pip and PC3flu cells were washed with PBS to remove the non-internalized NPs, and then irradiated with X-ray (Cs-137 with energy of 0.6616 Mev) at doses of 0, 2, 4, 6 and 8 Gy. Next, the cells were harvested, counted, and seeded into 6-well plates. After incubating for 10 days, the cells were washed with PBS, fixed with 4% paraformaldehyde and stained with 0.4% crystal violet. The colony number was counted to calculate the surviving fraction. To determine the selective killing of PC3pip cells,

an additional set of experiments was designed. PC3pip and PC3flu cells were individually administered Au-Gd(III)-PSMA NPs, incubated, and washed. Following washing the cells were combined together at a 1:1 ratio. The mixed cell suspension was irradiated with 4 Gy and reseeded into a 6-well plate. Following an additional incubation of 10 days, Au-Gd(III)-PSMA NPs were added again to label the cells expressing PSMA receptor (incubated for 24 h) and silver staining was carried out to verify the PC3pip colonies and PC3flu colonies.

In vivo tumor targeting and MR imaging

All mice were handled and processed according to an approved protocol by Case Western Reserve University's IACUC (Animal Experimentation application 2015-003, approved 3/27/2018-3/27/2021). Nude mice with flank tumors, PC3pip tumor or PC3flu tumor, were used to evaluate the active targeting of Au-Gd(III)-PSMA NPs and MR imaging. Mice (n = 3) were injected (i.v.) with Au-Gd(III)-PSMA NPs at 60 μmol Gd(III)/kg body weight. Mice were imaged by MR on a Bruker Biospin 7 T magnet (Bruker Biospin, Billerica, MA, U.S.A.) before and 0.5 h, 1 h, 2 h, 3 h, 4 h, 6 h, 8 h and 24 h after injection using a spin echo sequence: TR = 500 ms, TE = 8.1 ms, flip angle = 180°, NEX = 3, FOV = 20 × 20 mm^2, slice thickness = 1 mm, and matrix size = 256 × 256. The CNR of tumors was calculated as following: CNR= (tumor mean intensity - muscle mean intensity)/noise. Mice were euthanized after MR scanning and organs were discretized, weighed, lyophilized and digested with nitric acid to analyze both Au and Gd(III) content using ICP-MS.

Radiation therapy

When the PC3pip tumor reached a size about 100 mm^3, mice were divided randomly into groups (n=5), which were injected with PBS, Au-Gd(III)-PSMA NPs or Au-Y(III)-PSMA NPs. Two different doses, 60 umol/kg and 30 umol/kg in terms of Gd(III) or Y(III), were injected (i.v.), and 4 hours after injection, the mice received 6 Gy of X-ray radiation focused onto the tumor area only. For another set of mice injected with either PBS or Au-Gd(III)-PSMA NPs (60 umol/kg), X-ray radiation (6 Gy) was given twice both at 4 h and 48 h after injection. All irradiated mice were monitored for tumor sizes and body weight every other day over 30 days.

Diffusion-weighted imaging (DWI)

DWI images were acquired for each mouse. Briefly, mice were anesthetized in soflurane and placed in the prone orientation at isocenter in a Bruker Biospec 7.0T MRI scanner. Mice were maintained at 35 +/- 1 degree Celsius and 40-60 breaths throughout the imaging procedure. Following initial localizer axial DWI images were obtained for each animal's tumor using a DWI-EPI (echo planar imaging) acquisition (TR/TE = 2000 / 27 ms. b = 0 and 500 s/mm^2, FOV = 17.6 x 16 mm, matrix = 110 x 100, slice thickness = 1mm, 3 signal averages, and 4 EPI segment / TR).

All raw data was exported for offline analysis in Matlab (The Mathworks, Natick, MA). Apparent Diffusion Coefficient (ADC) maps were obtained for each imaging slice using established mon-exponential models.[4,5] A region-of-interest analysis was then performed to measure the mean ADC value (in mm2/sec) for each tumor and imaging time point.

Statistics

All the experiments were performed in triplicates unless stated otherwise. All numerical results are expressed as mean±SD. Descriptive statistics and significant differences between groups were analyzed using two-tailed student's t-tests, and the difference was considered significant if *$p < 0.05$ and **$p < 0.01$.

References

1. Rotz, M. W.; Holbrook, R. J.; MacRenaris, K. W.; Meade, T. J., A Markedly Improved Synthetic Approach for the Preparation of Multifunctional Au-DNA Nanoparticle Conjugates Modified with Optical and MR Imaging Probes. *Bioconjugate Chem.* **2018,** *29*, 3544-3549.

2. Brust, M.; Walker, M.; Bethell, D.; Schiffrin, D. J.; Whyman, R. Synthesis of Thiol-derivatised Gold Nanoparticles in a Two-phase Liquid-Liquid System. *J. Am. Chem. Soc.* **1994**, 801-802.

3. Liu, J.; Duchesne, P. N.; Yu, M.; Jiang, X.; Ning, X.; Vinluan, R. D.; Zhang, P.; Zheng, J. Luminescent Gold Nanoparticles with Size-Independent Emission. *Angew. Chem. Int. Ed.* **2016**, 55, 8894-8898.

4. Goodnough, C. L.; Gao, Y.; Li, X.; Qutaish, M. Q.; Goodnough, L. H.; Molter, J.; Wilson, D.; Flask, C. A.; Yu, X. Lack of dystrophin results in abnormal cerebral diffusion and perfusion in vivo. *Neuroimage* **2014**, 102, 809-816.

5. Erokwu, B.; Flask, C.; Gulani, V. High field diffusion tensor imaging in small animals and excised tissue. *Methods Mol. Biol.* **2011**, 771, 139-152.

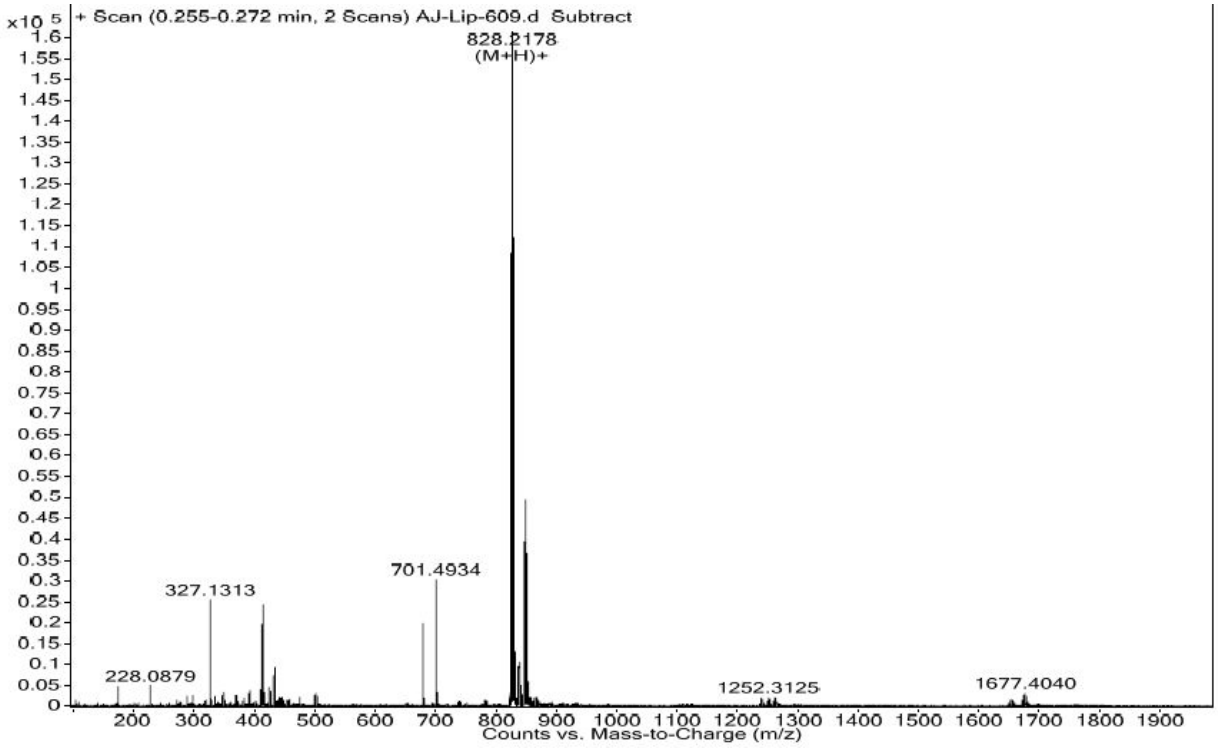

Figure S1. ESI Mass Spectrum of Dithioline-Gd(III) ligand at 828 (m/z).

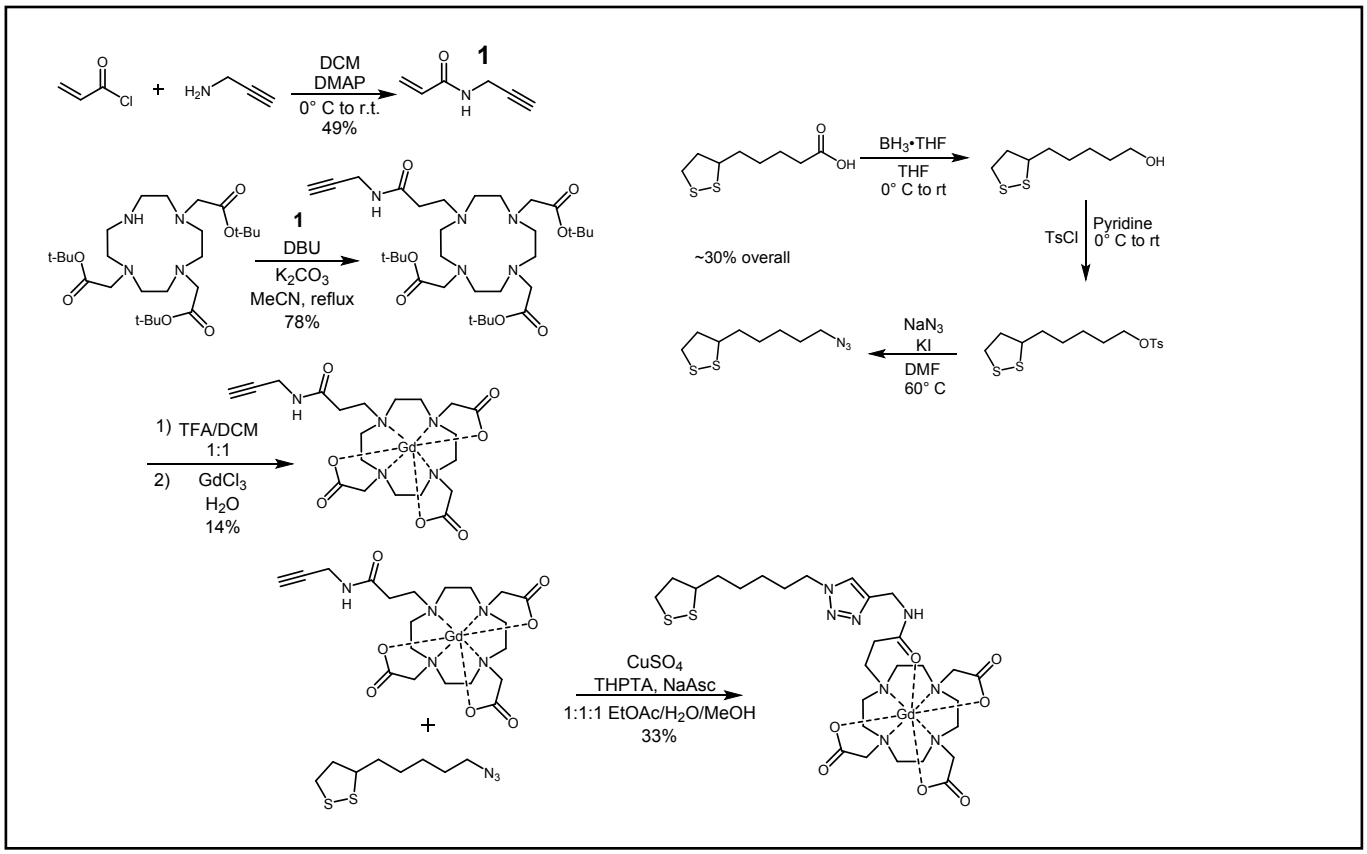

Figure S2. Convergent synthetic scheme for Dithioline-Gd(III) complex. The Y(III) complex was prepared in a similar fashion.

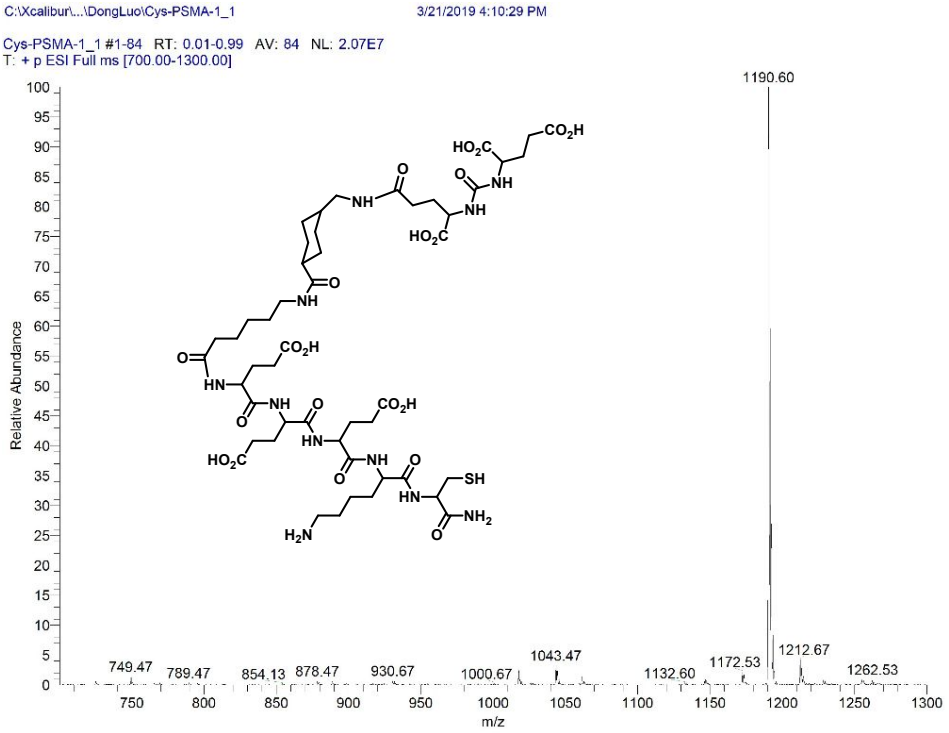

Figure S3. ESI mass spectrum of Cys-PSMA-1 ligand at 1190 (m/z).

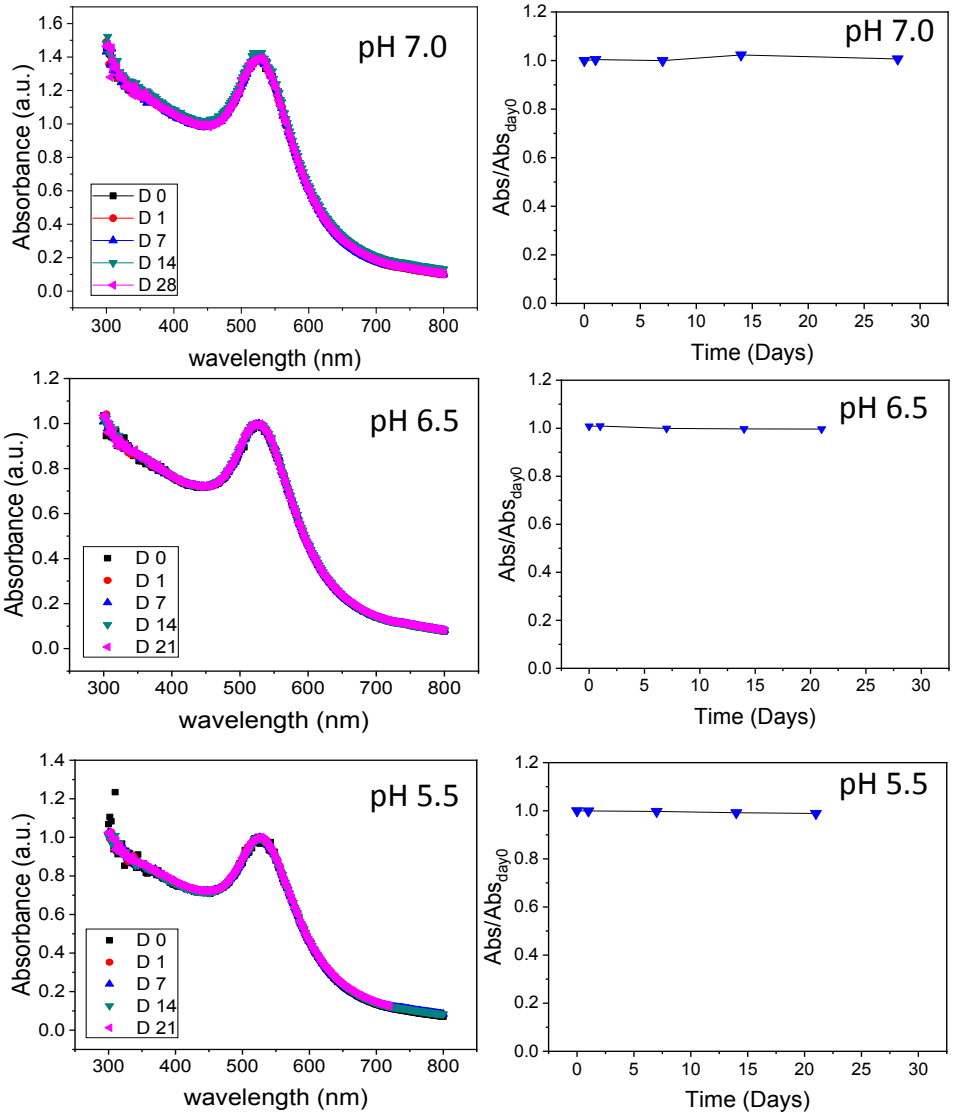

Figure S4. UV-Vis absorbance spectroscopy was employed to ascertain the stability of Au-Gd-PSMA NPs in 10% FBS solution (pH=7.0) and PBS (pH=6.5 and 5.5) by monitoring the surface plasmon resonance (SPR) band of gold (~520 nm). The data suggests that the nanoparticles are stable over at least 3 weeks with (left) no shift of absorbance band and (right) the absorbance intensity does not change significantly compared to that at day 0.

Table S1. Measured values of T_1 and corresponding [Gd(III)] measured by ICP-MS for Gd(III) complex

sample	[Gd]/mM	T_1 (ms)	T_1 (s)	$1/T_1$
1	0.5	330	0.33	3.03
2	0.25	575	0.575	1.73
3	0.125	1030	1.03	0.97
4	0.0625	1510	1.51	0.66
5	0.03125	2232	2.232	0.45

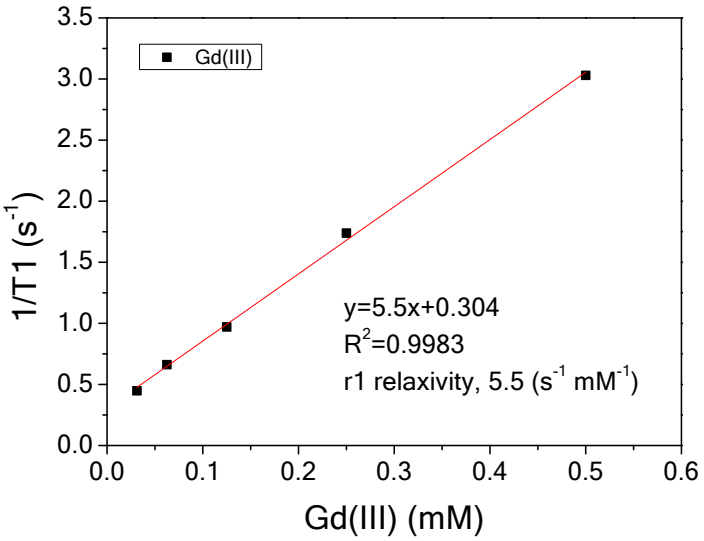

Figure S5. Example of r_1 relaxivity calculation for free Gd(III) complex.

Table S2. Measured values of T_1 and corresponding [Gd(III)] measured by ICP-MS for Au-Gd NPs

sample	[Gd]/mM	T_1 (ms)	T_1 (s)	$1/T_1$
1	0.258	116.5	0.1165	8.58
2	0.129	221.9	0.2219	4.51
3	0.0645	424.1	0.4241	2.358
4	0.0323	753.5	0.7535	1.327
5	0.0161	1315.5	1.3155	0.760

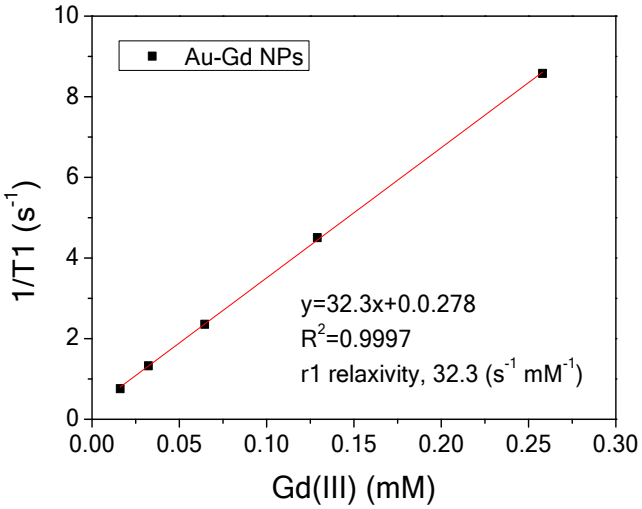

Figure S6. r_1 relaxivity calculation for free Au-Gd NPs.

Table S3. Measured values of T_1 and corresponding [Gd(III)] measured by ICP-MS for Au-Gd-PSMA NPs

sample	[Gd]/mM	T_1(ms)	T_1(s)	$1/T_1$
1	0.086	494.5	0.4945	2.022
2	0.043	874.5	0.8745	1.144
3	0.0215	1445	1.445	0.692
4	0.0108	2115	2.115	0.473
5	0.0054	2790	2.79	0.358

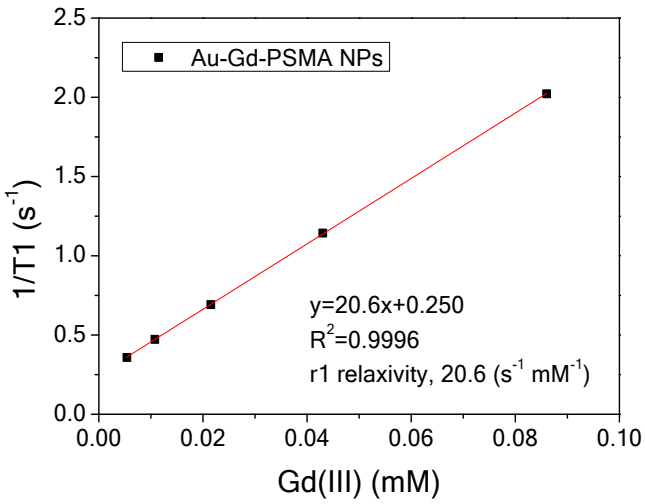

Figure S7. r_1 relaxivity calculation for free Au-Gd-PSMA NPs.

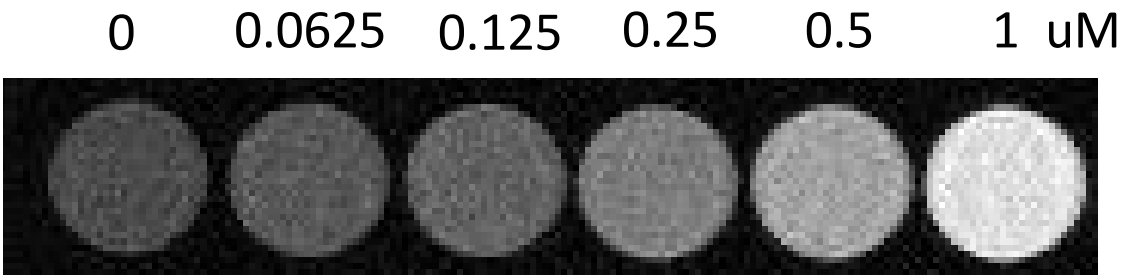

Figure S8. MRI Solution phantom of Au-Gd-PSMA NPs at different Gd(III) concentrations.

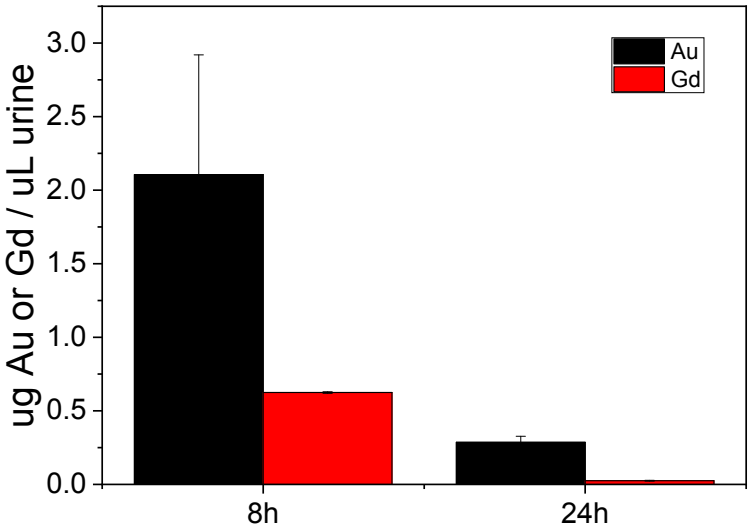

Figure S9. Au and Gd(III) content in collected urine samples at 8 h and 24 h post-injection of Au-Gd-PSMA NPs as determined by ICP-MS. Data are presented as mean ± SD (n = 3).

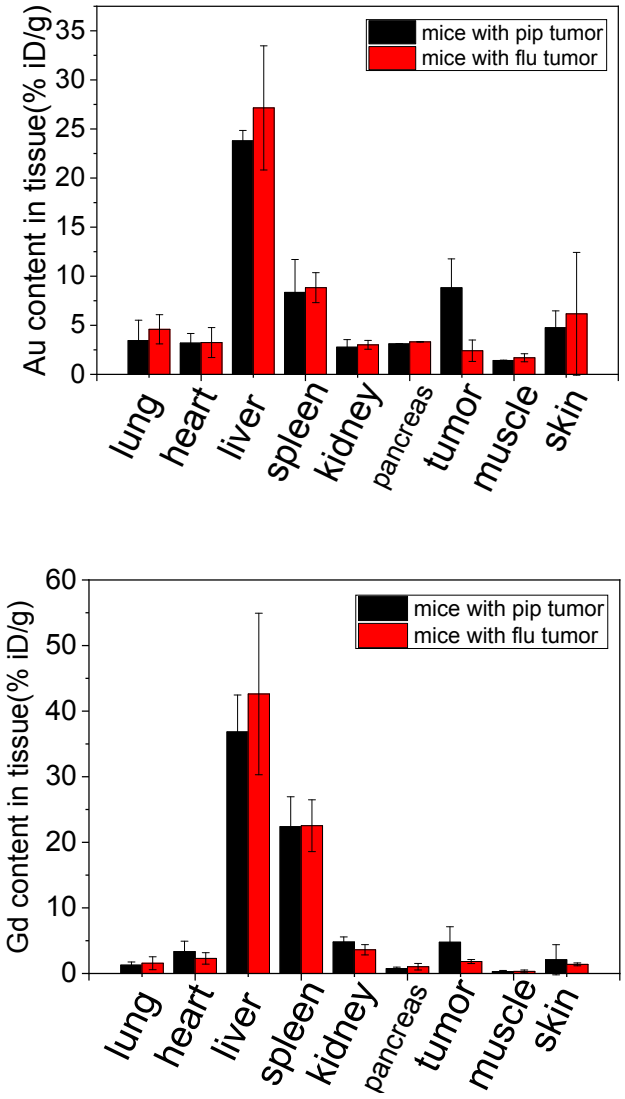

Figure S10. Au and Gd(III) content in main organs at 24 h post-injection of Au-Gd-PSMA NPs as determined by ICP-MS. Data are presented as mean ± SD (n = 3).

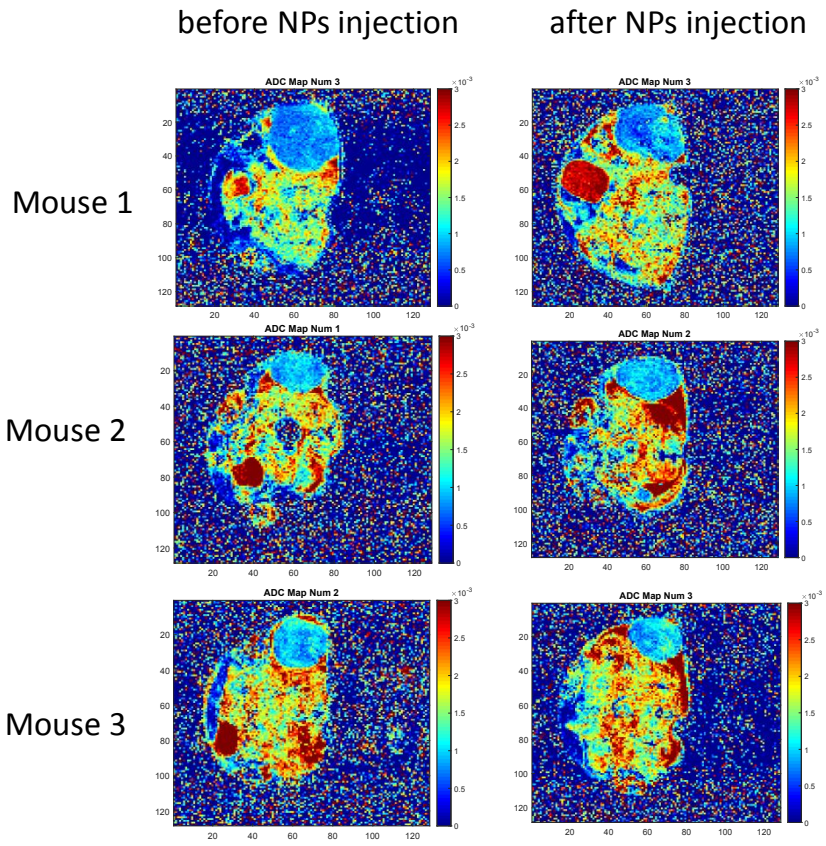

Figure S11. ADC maps of mice before and after injection of Au-Gd-PSMA NPs. NP injection does not affect the apparent diffusion coefficient of H_2O.